

Sliding friction in the hydrodynamic lubrication regime for a power-law fluid

Patrick B. Warren*

Unilever R&D Port Sunlight, Quarry Road East, Bebington, Wirral, CH63 3JW, UK.[†]

(Dated: February 4, 2015; July 9, 2023; published as J. Phys.: Cond. Matter **29**, 064005 (2016).)

A scaling analysis is undertaken for the load balance in sliding friction in the hydrodynamic lubrication regime, with a particular emphasis on power-law shear-thinning typical of a structured liquid. It is argued that the shear-thinning regime is mechanically unstable if the power-law index $n < 1/2$, where n is the exponent that relates the shear stress to the shear rate. Consequently the Stribeck (friction) curve should be discontinuous, with possible hysteresis. Further analysis suggests that normal stress and flow transience (stress overshoot) do not destroy this basic picture, although they may provide stabilising mechanisms at higher shear rates. Extensional viscosity is also expected to be insignificant unless the Trouton ratio is large. A possible application to shear thickening in non-Brownian particulate suspensions is indicated.

I. INTRODUCTION

Lubrication is usually considered to be a mechanical engineering problem [1–6], demanding sophisticated multi-scale numerical approaches for its solution [7–11]. However lubrication is also relevant for sensory physics, for example in understanding the origins of ‘mouth-feel’ and the sensory properties of foods [12, 13], and in ‘psycho-rheology’ and the perception of skin care products [14]. The lubricants in these sensory physics applications are often structured liquids or soft solids, with significant non-Newtonian rheologies. This raises the question how far traditional mechanical engineering lubrication theory can be used, and indeed whether new phenomena may be encountered. With this in mind, I present a scaling analysis of sliding friction in the hydrodynamic lubrication regime which extends to encompass the power-law shear thinning behaviour commonly encountered in structured liquids and complex fluids. The aim is to provide insights and guidance for these unconventional application areas, and motivate further work. Appendix B shows how the same approach can be used to recover a number of known results in squeeze-flow lubrication [15–17].

To begin with, let me outline the fundamental mechanism of pure hydrodynamic lubrication in sliding friction [18–20]. In a fully lubricated conjunction (Fig. 1), mass conservation within the converging and diverging wedges induces a Poiseuille-like contribution to the entrainment flow, superimposed on a Couette-type shearing motion. There is a corresponding emergent pressure distribution (Fig. 1b), which supports the load. The ratio of the load to the lateral sliding force defines the sliding friction coefficient μ . As we shortly shall see, Reynolds lubrication theory [1] predicts μ is proportional to the *Sommerfeld number* $S \equiv \eta UR/W$, where η is the lubricant viscosity, U is the sliding velocity, R is a length scale characterising

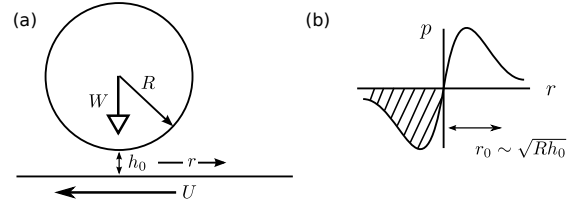


FIG. 1. Sliding friction between a sphere and flat. (a) It is supposed that the flat surface is sliding at a velocity U underneath the sphere. (b) The skew-symmetric Reynolds lubrication pressure distribution.

the curvature of the surfaces, and W is the normal load. The overall $\mu(S)$ behaviour is often summarised in the semi-empirical *Stribeck curve* (Fig. 2). Note that pure hydrodynamic lubrication breaks down as $S \rightarrow 0$ since the surfaces come into close contact, and one segues into a regime where elasto-hydrodynamic lubrication (EHL) is relevant, and ultimately into a regime of boundary lubrication (BL). This is reflected in the behaviour observed empirically in the Stribeck curve. The present scaling analysis does not incorporate EHL or BL, and should be interpreted within this wider context.

Before embarking on the detailed development, one further general remark should be made. In a geometry which possesses reflection symmetry, Reynolds lubrication theory predicts the lubrication pressure should be skew-symmetric about the minimum gap (Fig. 1b). Therefore, the integrated lubrication pressure should vanish. In actuality it has long been recognised that some additional physics intervenes to knock down this result. For instance in the trailing edge where the lubrication pressure is sub-ambient (shaded area in Fig. 1b), the free surface may separate [21], or the fluid may cavitate [22]. These considerations make the exact solution to the problem dependent on the nature of the additional physics. However a simple and commonly used prescription is to discard the contribution from the sub-ambient pressure region—this is the so-called half-Sommerfeld boundary condition [2]. I shall tacitly use this assumption below.

* patrick.warren@stfc.ac.uk

[†] Current address: The Hartree Centre, STFC Daresbury Laboratory, Warrington, WA4 4AD, United Kingdom

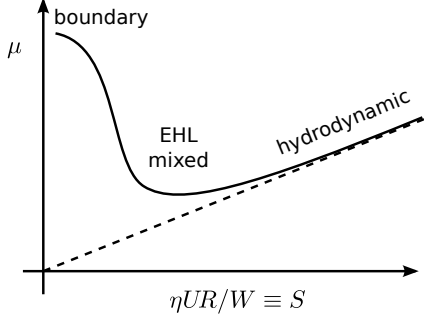


FIG. 2. Stribeck curve (friction coefficient as a function of Sommerfeld number). EHL is elasto-hydrodynamic lubrication. In the hydrodynamic regime (to which the present scaling analysis is applicable), the friction coefficient is proportional to the Sommerfeld number (dashed line).

Keeping all this in mind, in the next section I shall develop scaling arguments which recover the standard results for sliding friction in the hydrodynamic lubrication regime. In the following section I shall extend these to power-law fluids.

II. SCALING ANALYSIS: NEWTONIAN CASE

The gap between the lubricated surfaces, as shown in Fig. 1a for example, can be represented in the conjunction region by a parabolic profile

$$h = h_0 + \frac{r^2}{2R}. \quad (1)$$

In this h_0 is the minimum gap, r is the radial distance from the minimum gap, and R is a measure of the radius of curvature of the surfaces (*e.g.* the sphere radius in Fig. 1a). The radius within which h remains of order h_0 defines a length scale $r_0 \sim (Rh_0)^{1/2}$. This length scale sets the size of the conjunction region in terms of the Reynolds lubrication pressure distribution (Fig. 1b). With this insight one can easily calculate the mechanical properties of the conjunction such as the supported load and the tangential friction force. Thus the identification of r_0 is the key to the development of the scaling argument. This applies not only for sliding friction but also to squeeze-flow lubrication as discussed in Appendix B.

As already alluded to, and described in more detail in Appendix A, mass conservation induces a Poiseuille-type flow of magnitude U superimposed on the Couette-type shearing motion. The matching Reynolds lubrication pressure distribution is such that $U \sim (h_0^2/\eta)\nabla p$ where ∇p represents the magnitude of the pressure gradient. Note that the lubrication pressure develops in the radial direction, thus r_0 should be used as an estimate of the distance over which the pressure varies (Fig. 1b). Denoting

by p the magnitude of Reynolds lubrication pressure, the pressure gradient is therefore estimated by $\nabla p \sim p/r_0$. Putting these elements together, a scaling estimate of the magnitude of the lubrication pressure is given by

$$p \sim \frac{\eta U r_0}{h_0^2}. \quad (2)$$

As already outlined, the area of the conjunction in terms of the Reynolds lubrication pressure distribution is $r_0^2 \sim Rh_0$. Then the *integrated* pressure (*e.g.* the unshaded area in the Fig. 1b) corresponds to a normal force

$$pr_0^2 \sim \frac{\eta U r_0^3}{h_0^2} \sim \eta U R^{3/2} h_0^{-1/2}. \quad (3)$$

In this I have used $r_0 \sim (Rh_0)^{1/2}$ for the second step. Note that this force diverges as $h_0^{-1/2}$ as the gap shrinks ($h_0 \rightarrow 0$). The stable gap (see below) will be such that the integrated lubrication pressure supports the load. This happens when $pr_0^2 \sim W$, or alternatively, using Eq. (3), when

$$\frac{h_0}{R} \sim \left(\frac{\eta U R}{W} \right)^2 \quad (\sim S^2). \quad (4)$$

More careful treatments restore a prefactor to this, for example Kapitza [21] derived $h_0/R = (72\pi^2/25)S^2 \approx 28.4S^2$, and Hamrock [2] has $h_0/R \approx 34.8S^2$.

A point not often stressed, but which will be critical in the sequel, is that the lubricated conjunction is indeed *mechanically stable* at the load balance condition. To see this suppose that the minimum gap h_0 has not yet taken its steady state value. The load W bears down on the conjunction, and is opposed by the lubrication pressure which exerts a force of order pr_0^2 given by Eq. (3). However as already mentioned $pr_0^2 \sim h_0^{-1/2}$. Therefore if the gap is too large, the lubrication pressure does not support the load and the gap closes. Conversely, if the gap is too small, the lubrication pressure overcompensates for the load and the gap opens up. This stabilising mechanism is shown schematically in Fig. 3, where the solid line is the normal force arising from the lubrication pressure. In the language of dynamical systems theory, the filled circle in this diagram is a *stable fixed point*.

I turn now to the Stribeck curve. Since the shear rate $\dot{\gamma} \sim U/h_0$ the tangential wall stress in the conjunction zone is of order $\eta\dot{\gamma} \sim \eta U/h_0$ (see Appendix A for a more careful justification of this). Multiplying by the area of the conjunction ($\sim r_0^2$) gives the tangential force $T \sim \eta U r_0^2/h_0$. Hence the friction coefficient

$$\mu \equiv \frac{T}{W} \sim \frac{\eta U r_0^2}{W h_0} \sim \frac{\eta U R}{W} \quad (\sim S) \quad (5)$$

(using the geometrical condition $r_0^2 \sim Rh_0$). This now explains why $\mu \propto S$ in the hydrodynamic part of the Stribeck curve. Note that the gap shrinks as $h_0 \sim S^2$ from Eq. (4). As S decreases (*i.e.* low velocity, high load) eventually the gap becomes very small and the friction coefficient deviates from the pure hydrodynamic law at the point where one enters the EHL/BL regime.[23]

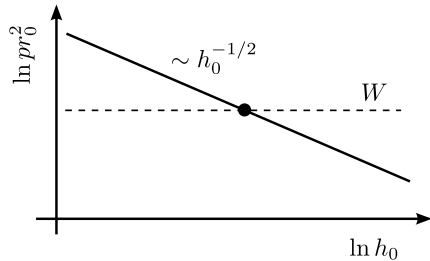


FIG. 3. Load curve in the Newtonian case. The solid line is the normal force generated by the lubrication pressure. The filled circle is a stable fixed point, under a given load.

III. POWER-LAW FLUIDS

I now propose the obvious extensions of the above scaling arguments to incorporate non-linear rheological effects of interest found in structured liquids and complex fluids. For the time being I shall leave aside the question of normal stress, flow transience, and extensional flow, and focus first on the typical power-law shear thinning found in these systems.

A. Shear thinning

I shall represent the non-linear viscosity in this case by a simple model, *cf.* [11],

$$\eta = \frac{\eta_0}{1 + (\dot{\gamma}\tau)^\alpha}. \quad (6)$$

This model describes a power-law fluid with a low shear (first) Newtonian plateau. In Eq. (6) η_0 is the low shear viscosity (*i.e.* in the Newtonian plateau), $\dot{\gamma}$ is the shear rate, τ is a characteristic relaxation time, and α is an exponent characterising the rate of decrease of the viscosity in the shear-thinning regime. In the shear-thinning regime, the shear stress $\eta\dot{\gamma} \sim \dot{\gamma}^{1-\alpha}$, thus we identify the power-law index $n = 1 - \alpha$. The analysis below will be undertaken largely in terms of α , but the results will also be presented in terms of statements about the power-law index. For concreteness, a typical value of the exponent for polymer melt rheology is $\alpha \approx 0.8$ –1 [24–26] (power-law index $0 \lesssim n \lesssim 0.2$). One should note that $\alpha = 1$ (which would correspond to a plateau in the shear stress) is nowadays usually taken to be a signal of shear banding [27].

The dimensionless quantity $\dot{\gamma}\tau$ in Eq. (6) is the *Weissenberg number* and is a measure of the extent to which the non-linear regime has been penetrated. Eq. (6) omits the second Newtonian plateau which is expected to obtain at very high shear rates; this will be added informally in a moment.

Inserting Eq. (6) into Eq. (3) gives a revised estimate for the normal force produced by the lubrication pressure,

$$pr_0^2 \sim \frac{\eta_0}{1 + (\dot{\gamma}\tau)^\alpha} \times UR^{3/2}h_0^{-1/2} \quad (7)$$

where the shear rate is estimated by $\dot{\gamma} \sim U/h_0$. The assumptions being made here will be reviewed later. Since $\dot{\gamma} \sim 1/h_0$, there are two regimes. For large gap, the Weissenberg number is small ($\dot{\gamma}\tau \lesssim 1$) and one recovers the Newtonian behaviour seen already, with $\eta = \eta_0$ being the viscosity in the first Newtonian plateau.

For small gap, one enters the high Weissenberg number regime ($\dot{\gamma}\tau \gtrsim 1$) in which case Eq. (7) becomes

$$pr_0^2 \sim \eta_0(\dot{\gamma}\tau)^{-\alpha} UR^{3/2}h_0^{-1/2} \sim h_0^{\alpha-1/2} \quad (\sim h_0^{1/2-n}). \quad (8)$$

Only the h_0 -dependence has been retained in the final step. If $\alpha < 1/2$ (weak shear thinning, power-law index $n > 1/2$), then pr_0^2 in Eq. (8) diverges as $h_0 \rightarrow 0$ and one would again expect the gap to be mechanically stable, albeit with a modified dependence on the Sommerfeld number. On the other hand, if $\alpha > 1/2$ (strong shear thinning, power-law index $n < 1/2$), pr_0^2 in Eq. (8) is an *vanishing* function of h_0 as $h_0 \rightarrow 0$ and therefore the load balance in this regime will be *unstable*.

I shall take this latter case (strong shear thinning, power-law index $n < 1/2$) to be the one of most interest. The two regimes in the load balance are illustrated in Fig. 4a. The left hand branch is the high Weissenberg number regime where shear thinning takes place. In this branch, the open circle corresponds to an unstable fixed point at load W_1 . To the left of the open circle, the lubrication pressure is insufficient to support the load and the gap closes until interrupted by some additional physics. To the right of the open circle, the lubrication pressure forces the surfaces to move apart until one reaches the stable fixed point (filled circle) in the low Weissenberg number regime. Now consider increasing the load to W_2 . In this situation, the lubrication pressure is *never* sufficient to keep the surfaces apart and the gap closes until one enters the mixed or boundary layer lubrication regime. Somewhere in between W_1 and W_2 is a critical load at which the stable and unstable fixed points merge in a saddle-node bifurcation.

The implication for the Stribeck curve is as follows. In the low Weissenberg number regime, the analysis goes through as for the Newtonian case, with η_0 featuring as the viscosity. The Weissenberg number $\dot{\gamma}\tau \sim S^{-2}$, and increases as the Sommerfeld number shrinks. Mechanical stability is lost at the point where one enters the shear thinning regime (*i.e.* at the saddle-node bifurcation). At this point the surfaces should jump into (near) contact. Correspondingly the Stribeck curve should show a discontinuous jump (Fig. 4b).

If one envisages that a second Newtonian plateau appears at very high shear rates, then a restabilisation mechanism emerges naturally. In this situation, the expected behaviour of the lubrication pressure is shown in

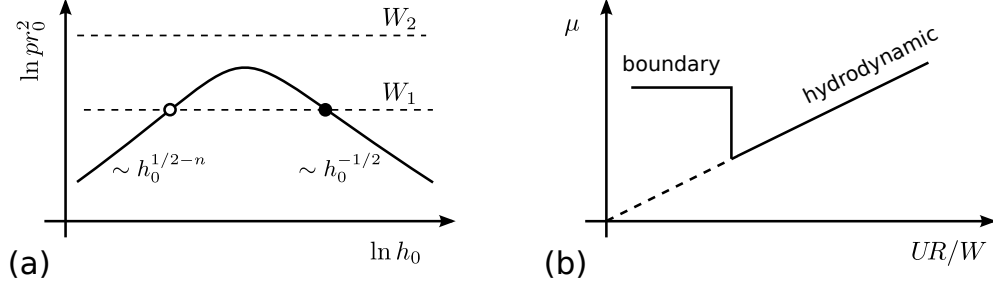


FIG. 4. (a) Load curves in the non-Newtonian strong shear thinning case (power-law index $n < 1/2$). The solid line is the normal force generated by the lubrication pressure. A filled (open) circle is a stable (unstable) fixed point, under a given load. The fixed points disappear in a saddle-node bifurcation as the load is increased. (b) The corresponding Stribeck curve is predicted to jump discontinuously at the critical load, perhaps into a boundary lubrication regime.

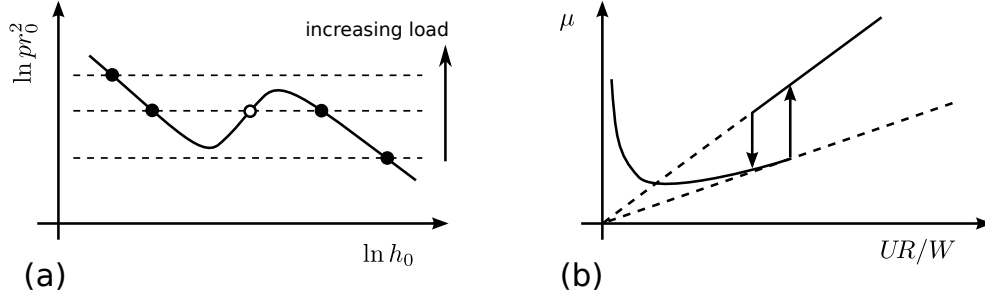


FIG. 5. (a) Lubrication pressure in the case of shear thinning with a second Newtonian plateau. (b) Consequential hysteresis in the Stribeck curve.

Fig. 5a. Consider increasing the load, starting from a small value. At first one follows the right hand branch of the pressure curve, until stability is lost at the upper saddle-node bifurcation and the system jumps onto the left hand branch. Subsequently decreasing the load reverses the process, except that the jump back occurs at the lower saddle-node bifurcation. The corresponding Stribeck curve displays *hysteresis* and can be constructed by noting that the stable fixed points lie on branches of the lubrication pressure curve where the flow is Newtonian. This is illustrated in Fig. 5b.

B. Normal stress

Let me now consider some of the other non-linear rheological effects that might be relevant for non-Newtonian lubricants. A long standing question which can be addressed in the context of the scaling analysis is the rôle of normal stress. Again, a simple model capturing this is

$$N = \frac{\psi_0 \dot{\gamma}^2}{1 + (\dot{\gamma}\tau)^\beta} \quad (9)$$

where $\psi_0 \sim \eta_0 \tau$ is a normal stress coefficient and β is another exponent. For concreteness, a typical value of this exponent is $\beta \approx 1.3\text{--}1.5$ for polymer melts [24–26].

The contribution that normal stress makes to the load balance can be found by multiplying by the area of the conjunction, $r_0^2 \sim R h_0$. Alternatively we can just compare the normal stress with the Reynolds lubrication pressure. In the low Weissenberg number regime ($\dot{\gamma}\tau \lesssim 1$) the ratio of these two is

$$\frac{N}{p} \sim \frac{\psi_0 \dot{\gamma}^2}{\eta_0 U r_0 / h_0^2} \sim \dot{\gamma}\tau \times \frac{h_0}{r_0}. \quad (10)$$

where the pressure has been taken from Eq. (2), and $U \sim \dot{\gamma} h_0$ and $\psi_0 \sim \eta_0 \tau$ have been substituted in the final step. The last factor $h_0/r_0 \sim (h_0/R)^{1/2}$ is expected to be a small number (*e.g.* $\lesssim 0.1$, say), so the ratio N/p is expected to remain small in the $\dot{\gamma}\tau \lesssim 1$ regime. In particular normal stress should not affect the situation in the stable lubrication flow up until the loss of stability at the saddle-node bifurcation in Fig. 4. Therefore the overall picture shown in Fig. 4 remains unchanged.

In the high Weissenberg number regime ($\dot{\gamma}\tau \gtrsim 1$) one has $N r_0^2 \sim h_0^{\beta-1}$. As long as $\beta > 1$ this is an increasing

function of h_0 , and the gap remains mechanically unstable in this regime. Only if $\beta < 1$ will normal stress rescue the conjunction from complete mechanical collapse by providing enough normal force to support the load in a stable sliding configuration. However since I have argued normal stress does not affect the loss of mechanical stability at the saddle-node bifurcation, one would not expect this stabilising mechanism to become relevant until well into the non-linear regime. Therefore, one would still expect hysteresis in the Stribeck curve.

C. Flow transience

Another factor that can be considered is that the flow is transient on a time scale of order the transit time $t_s \sim r_0/U$. The dimensionless ratio $\tau/t_s \sim U\tau/r_0$ is known as the *Deborah number*, and its magnitude gives an indication of the importance of transient flow effects, such as stress overshoot. Substituting $U \sim \dot{\gamma}h_0$ shows that the Deborah number is of the order $\dot{\gamma}\tau \times h_0/r_0$. This is the same as the ratio N/p for the normal stress above, and the same argument goes through so that the overall picture remains unchanged. Like normal stress, it is possible that transient flow effects may grow to become significant in the non-linear regime since the Deborah number scales as $h_0^{-1/2}$. Hence this may provide another mechanism to re-stabilise the gap at a smaller distance.

D. Extensional viscosity

In Appendix A, the ratio of the extension to the shear components in the lubrication flow is estimated to be of the order $(h_0/R)^{1/2}$. This is the same small number encountered above, and here should be compared to the *Trouton ratio* (*i.e.* between extensional and shear viscosity). For example, for polymer melts the Trouton ratio is of the order 3 in the low Weissenberg number regime (where the gap is stable), and does not increase much in the non-linear regime [24]. On these grounds one would not expect extensional viscosity to affect the friction curve, but the situation may have to be re-evaluated if the Trouton ratio is large.

IV. DISCUSSION

The main result is that for sliding friction in the hydrodynamic regime with a strongly shear thinning lubricant (power-law index $n < 1/2$) the conjunction is predicted to become mechanically unstable at the point where the shear thinning regime is entered. This is because in the shear-thinning regime, with $n < 1/2$, the integrated Reynolds lubrication pressure *diminishes* as the gap shrinks, and is therefore unable to support the load. The gap should therefore collapse until some other physics intervenes. This would lead to a discontinuous jump in the

Stribeck (friction) curve as the load is increased (Fig. 4b). Non-linear effects such as normal stress and flow transience are estimated to be subdominant at the point of entry into the non-linear regime, so it is unlikely they would destroy the basic picture although they may provide stabilising mechanisms at high shear rates. Extensional viscosity is also estimated to be insignificant unless the Trouton ratio is large (say, $\gtrsim 10$). Depending on the nature of the restabilising mechanism at small gaps, the Stribeck curve may show hysteresis (Fig. 5b).

These results were established on the back of scaling arguments which involve perhaps naïve and rather drastic assumptions. For example, the lubrication flow is assumed to remain essentially the same as in the Newtonian case, but with a substituted shear-rate dependent viscosity $\eta(\dot{\gamma})$. If this breaks down (for example due to a non-linear superimposition of the Poiseuille and Couette flows) the analysis would be invalid. Furthermore, very simple models were taken for the shear viscosity and normal stress as a function of shear rate, and additivity of the normal stress and lubrication pressure was assumed. There are certainly available much more sophisticated (tensor) constitutive models, such as the Rolie-Poly equation for polymer melts [26], or the phenomenological White-Metzner model [28]. An important avenue for future work is to investigate more thoroughly the properties of Reynolds lubrication flow using such constitutive models. An intriguing possibility is that the non-linear rheology could break the reflection symmetry in the lubrication pressure profile (Fig. 1b), thus relieving the theory of the necessity to appeal to some unstated physics to generate a resultant normal force.

The possible hysteresis in the Stribeck curve makes an interesting connection with recent theories of the microscopic origins of shear thickening in non-Brownian suspensions [29–31]. In these theories the shear thickening transition is associated with a ‘breakthrough’ to frictional contacts, and indeed the simulations in Fernandez *et al.* [29] are based on a discontinuous friction curve of exactly the form shown in Fig. 4b. Of course, the non-Brownian particles that show the phenomenon are more typically suspended in a Newtonian solvent, and not a structured liquid, and therefore one can question the relevance of the present analysis. Nevertheless, experimental systems are often prepared with polymer additives (as in [29]), and as such they may perhaps exhibit non-linear frictional behaviour of the kind described here if significant polymer adsorption occurs.

I thank M. J. Adams and S. A. Johnson for useful discussions, and critical reading of early versions of the manuscript.

Note added (July 2023): in relation to this problem what is commonly called ‘normal’ stress is actually manifest as a tensile ‘hoop’ stress (as in the rod-climbing effect) and so does not *directly* contribute to supporting a load in a sliding geometry. This re-inforces the conclusion that normal stress cannot stop a conjunction from becoming unstable in sliding, but makes the mechanism

by which it could rescue the conjunction from complete collapse at high Weissenberg number rather indirect: a full study remains an open problem to my knowledge. I thank Alexander Morisov for drawing my attention to this point.

Appendix A: Aspects of Reynolds lubrication flow

For a conjunction between non-conformal surfaces (cf. Fig. 1a), mass conservation implies that entrainment involves a superimposition of Couette and Poiseuille flows. The full solution requires numerics [2] but basic insights can be gained by considering the quasi-one-dimensional case [20]. In that case the flow is

$$v_x = -\frac{U}{h}(h-y) - \frac{1}{2\eta}\frac{dp}{dx}y(h-y). \quad (\text{A1})$$

Here x (cf. r) measures the distance along the gap, y measures the distance from the lower surface (moving at velocity $-U$), h is the gap (weakly varying with x), p is the Reynolds lubrication pressure, and η the viscosity. This velocity field corresponds to a net material flux

$$Q = \int_0^h v_x dy = -\frac{Uh}{2} - \frac{h^3}{12\eta}\frac{dp}{dx}. \quad (\text{A2})$$

This has to be constant, even though h varies, and is of order Uh_0 . The implication is that $(h_0^3/12\eta) dp/dx \sim Uh_0$, which gives an order of magnitude estimate of the pressure gradient. The associated Poiseuille flow velocity (along the centerline for instance) is then $(h_0^2/\eta) dp/dx \sim U$, as utilised in the main discussion.

The shear rate at the lower surface is

$$\left.\frac{\partial v_x}{\partial y}\right|_{y=0} = \frac{U}{h} - \frac{h}{2\eta}\frac{dp}{dx}. \quad (\text{A3})$$

Since $dp/dx \sim \eta U/h_0^2$, the two terms are comparable, and the wall stress can be estimated by $\eta U/h_0$. This give rise to the friction force in hydrodynamic lubrication.

The flow field in Eq. (A1) is predominantly in the longitudinal direction. Differentiating with respect to this direction yields an estimate for the extensional component. This yields a number of terms, all of which are of the order $U/h \times dh/dx$. Since $h = h_0 + x^2/2R$ (cf. Eq. (1)), one has $dh/dx = x/R$, and setting $x \sim x_0 \sim (h_0 R)^{1/2}$ and $h \sim h_0$ gives U/x_0 for the magnitude of the extensional strain rate. This agrees with the simple picture that entrainment involves of the order 100% extensional strain, in a distance of the order x_0 , on a time scale of the order the transit time x_0/U . Hence the extensional strain rate $U/x_0 \sim (U/h_0) \times (h_0/x_0) \sim \dot{\gamma} \times (h_0/R)^{1/2}$. This is the origin of the estimate used in the main text.

Appendix B: Squeeze-flow lubrication

Scaling arguments along the lines of the main text can also be developed for squeeze-flow lubrication. In this

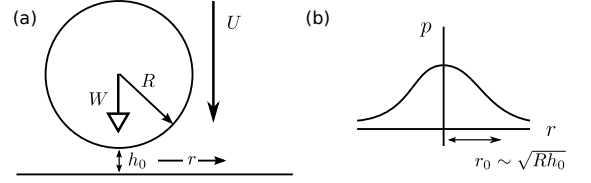


FIG. 6. Squeeze-flow lubrication between a sphere and flat. (a) The sphere approaches the flat surface at a velocity U . (b) The radially-symmetric Reynolds lubrication pressure distribution.

way one recovers number of known results [6, 15–17], which may help prove the *bona fides* of the approach. The main difference between squeeze-flow and sliding friction lies in the estimate of the radial flow rate u_r . Here, mass conservation in the conjunction zone (Fig. 6a) means that $Ur_0^2 \sim u_r r_0 h_0$, and therefore $u_r \sim r_0 U/h_0$ (cf. $u_r \sim U$ for the sliding friction case). Thus in squeeze-flow lubrication the radial flow rate is amplified by a factor r_0/h_0 compared to sliding case. From here, the development proceeds exactly as in the main text. The radial flow corresponds to a pressure gradient such that $(h_0^2/\eta)\nabla p \sim u_r \sim r_0 U/h_0$. The pressure gradient is estimated in terms of the magnitude of the Reynolds lubrication pressure by $\nabla p \sim p/r_0$. Finally, the normal force is estimated by pr_0^2 . When all this is put together,

$$pr_0^2 \sim \frac{\eta r_0^4 U}{h_0^3}. \quad (\text{B1})$$

Although ‘sans’ prefactor, this is actually a very old result due to Stefan [6]. At this point we have not yet used the geometric relation $r_0 \sim \sqrt{Rh_0}$. If this is inserted, we obtain

$$pr_0^2 \sim \frac{\eta R^2 U}{h_0}. \quad (\text{B2})$$

This is the classic Reynolds squeeze-flow lubrication force; a more careful treatment yields the exact result that the normal force $F = 3\pi\eta R^2 U/2h_0$ [2]. Note that the Reynolds lubrication pressure is radially symmetric in this case (Fig. 6b), and there is no need to appeal to hidden physics as in the half-Sommerfeld boundary condition.

The shear rate in the gap is estimated as $\dot{\gamma} \sim u_r/h_0 \sim r_0 U/h_0^2 \sim R^{1/2} U/h_0^{3/2}$. For power-law shear-thinning with $\eta \sim \dot{\gamma}^{-\alpha}$ we find (omitting the intermediate steps) the normal force

$$pr_0^2 \sim h_0^{3\alpha/2-1} \quad (\sim h_0^{(1-3n)/2}). \quad (\text{B3})$$

If $\alpha > 2/3$ (power-law index $n < 1/3$), this no longer diverges as $h_0 \rightarrow 0$. This signals that the force is controlled by the outer-region flow (on the length scale $\sim R$). This rather striking result was first reported by Rodin [16],

and later confirmed by Lian *et al.* [17]. In a sense, this is the analogue of the main text observation that for sufficiently strong shear thinning, the conjunction fails to support a load. The difference in the cross-over exponent value can be traced to the geometric amplification of the radial flow rate in the present situation.

The effect of normal stress can be assessed in the same way. Only the main results are summarised. First, in the low Weissenberg number regime one concludes that normal stress will be small compared to the Reynolds

lubrication pressure. Second, in the high Weissenberg number regime one finds that $N/p \sim h_0^{3(\beta-\alpha)/2-1}$. This diverges as $h_0 \rightarrow 0$ if $\beta < \alpha + 2/3$. This is a distinct possibility for the exponent values typical of a structured liquid and would mean that normal stress *is* relevant for squeeze-flow lubrication in the high Weissenberg number regime. A more detailed investigation of this possibility is left for future work.

-
- [1] J. A. Williams, *Engineering Tribology* (OUP, Oxford, 1994).
 - [2] B. J. a. Hamrock, *Fundamentals of Fluid Film Lubrication* (McGraw-Hill, New York, 1994).
 - [3] B. N. J. Persson, *Sliding Friction: Physical Principles and Applications* (Springer-Verlag, Berlin, 2000).
 - [4] J. A. Greenwood, Proc. Instn. Mech. Engrs.: Part J **214**, 29 (2000).
 - [5] S. Bair, P. Vergne, and M. Marchetti, Tribology Trans. **45**, 330 (2002).
 - [6] J. Engmann, C. Servais, and A. S. Burbidge, J. Non-Newtonian Fluid Mech. **132**, 1 (2005).
 - [7] C. Yang, U. Tartaglino, and B. N. J. Persson, Eur. Phys. J. E **19**, 47 (2006).
 - [8] J. H. Choo, H. A. Spikes, M. Ratoi, R. Glovnea, and A. Forrest, Trib. Int. **40**, 154 (2007).
 - [9] J. Y. Jang, M. M. Khonsari, and S. Bair, Proc. R. Soc. A **463**, 3271 (2007).
 - [10] P. Anuradha and P. Kumar, J. Eng. Tribology **225**, 173 (2011).
 - [11] B. N. J. Persson and M. Scaraggi, Eur. Phys. J. E **34**, 113 (2011).
 - [12] J. R. Stokes, L. Macakova, A. Chojnicka-Paszun, C. G. de Kruif, and H. H. J. de Jongh, Langmuir **27**, 3474 (2011).
 - [13] J. Chen and J. R. Stokes, Trends Food Sci. Technol. **25**, 4 (2012).
 - [14] S. Guest, F. McGlone, A. Hopkinson, Z. Schendel, K. Blot, and G. Essick, J. Cosmetics Dermat. Sci. App. **3**, 66 (2013).
 - [15] P. J. Leider and R. B. Bird, Ind. Eng. Chem. Fundamen. **13**, 336 (1974).
 - [16] G. Rodin, J. Non-Newtonian Fluid Mech. **63**, 141 (1996).
 - [17] G. Lian, Y. Xu, W. Huang, and M. J. Adams, J. Non-Newtonian Fluid Mech. **100**, 151 (2001).
 - [18] G. K. Batchelor, *An Introduction to Fluid Dynamics* (CUP, Cambridge, 1967).
 - [19] T. E. Faber, *Fluid Dynamics for Physicists* (CUP, Cambridge, 1995).
 - [20] E. Guyon, J.-P. Hulin, L. Petit, and C. D. Matescu, *Physical Hydrodynamics* (OUP, Oxford, 2001).
 - [21] P. L. Kapitza, Zh. Tekh. Fiz. **25**, 747 (1955).
 - [22] J. Ashmore, C. del Pino, and T. Mullin, Phys. Rev. Lett. **94**, 124501 (2005).
 - [23] Repeating these arguments for a two-dimensional geometry (*e.g.* a cylinder and flat) finds $\mu \sim S^{1/2}$ and $h_0/R \sim S$, where the Sommerfeld number $S = \eta U/W_L$, and W_L is the load per unit length.
 - [24] M. Doi and S. F. Edwards, *The Theory of Polymer Dynamics* (Clarendon, Oxford, 1986).
 - [25] R. S. Graham, A. E. Likhtman, T. C. B. McLeish, and S. T. Milner, J. Rheol. **47**, 1171 (2003).
 - [26] A. E. Likhtman and R. S. Graham, J. Non-Newtonian Fluid Mech. **114**, 1 (2003).
 - [27] T. Divoux, M. A. Fardin, S. Manneville, and S. Lerouge, Ann. Rev. Fluid Mech. **48**, 81 (2016).
 - [28] J. L. White and A. B. Metzner, J. Appl. Polym. Sci. **7**, 1867 (1963).
 - [29] N. Fernandez, R. Mani, D. Rinaldi, D. Kadau, M. Mosquet, H. Lombois-Burger, J. Caayer-Barrioz, H. J. Herrmann, N. D. Spencer, and L. Isa, Phys. Rev. Lett. **111**, 108301 (2013).
 - [30] R. Seto, R. Mari, J. F. Morris, and M. D. Denn, Phys. Rev. Lett. **111**, 218301 (2013).
 - [31] M. Wyart and M. E. Cates, Phys. Rev. Lett. **112**, 098302 (2014).